Chirality and Encapsulation Properties of Disubstituted Ferrocene−Peptide Dendrimers

Francis E. Appoh, Donald S. Thomas, and Heinz-Bernhard Kraatz*

Department of Chemistry, University of Saskatchewan, 110 Science Place, Saskatoon, SK, S7N 5C9, Canada

Received March 9, 2006; Revised Manuscript Received June 12, 2006

ABSTRACT: The synthesis and spectroscopic characterization of novel disubstituted glutamic acid dendrimers constructed on a ferrocene core are reported. The strong intramolecular hydrogen bonding observed in monosubstituted variants of the currently studied dendrimers is also observed for the disubstituted systems. DMSO is found to selectively disrupt this hydrogen bonding. The absence of any redox activity in generations 5 and 6 demonstrates the complete encapsulation of the ferrocene core.

Introduction

Conceptually, dendrimers can be viewed as a class of well-defined monodisperse polymers with a globular structure.[1,2] The size of higher generation dendrimers approaches that of small proteins, and in fact, these systems have been used to mimic some of the properties of proteins. In this context, the site isolation in dendrimers is of particular interest. The dendritic shell is able to encapsulate the functional core to create specific site-isolated nanoenvironments, thereby affecting molecular properties of the core. In particular for dendrimers having redox-active cores, the effect of the dendritic sheath on the electronic properties of the central redox core remains an active area of research. There are several studies available focusing on encapsulation of a central redox core by the dendrimer. However, there are often conflicting trends in the redox potential reported. In the case of Kaifer's dendrimers,[3−5] a central ferrocene (Fc) group is linked to a dendrimer via an amide linkage. The redox potential exhibits interesting influences as a function of dendrimer size and exterior dendrimer surface. While ester-terminated dendrimers in an organic solvent exhibit a shift to lower potential of the Fc core, the redox potential for the hydrophilic acid-terminated dendrimers increases with increasing generation in water. In the case of Smith's TRIS-based dendrimers, the dendrons act as a nonpolar shield which effectively encapsulated the Fc core and prevents ion penetration into the core.[6] Importantly, this hinders the oxidation of the central Fc core; thereby, it destabilizes oxidation to Fc^+, causing significant anodic shifts in the Fc redox potential. Similar anodic shifts with increasing dendrimer generation were reported by Thayumanavan's disubstituted Fc−benzyl ether dendrimers,[7,8] and Ashton's disubstituted Fc−carbohydrate dendrimers[9] exhibited anodic shifts with increasing generations.

We recently reported the synthesis of monosubstituted Fc core−glutamic acid ester dendrimers up to G6 using a convergent peptide coupling.[10] Intramolecular H-bonding in these peptide dendrimers enables the dendrons to fold in on themselves, resulting in structurally well-defined globular structure, which in turn shields the central core, influencing its redox properties. Electrochemical study showed only small cathodic shifts and an incomplete encapsulation even for G6. As a logical next step, it was decided to investigate the properties of disubstituted Fc−dendrimer systems and compare their properties to the monosubstituted Fc analogues. Can complete encapsulation be achieved for disubstituted Fc−peptide dendrimers? Does the growing dendimer sheath cause small cathodic shifts as was observed for the monosubstituted Fc systems? It is important for the understanding of the disubstituted Fc−peptide dendrimers to know that in general disubstituted Fc−peptides adopt a 1,2′-conformation of the Fc group having P-helicity if the peptide is derived from L-amino acids. For D-amino acids, the Fc group adopts a 1,5′-conformation, and the axial chirality of the Fc core is D-helical.[11−14] The "Herrick conformation" is stable in solution and the solid state. We speculated that disubstituted Fc−peptide dendrimers may display a dendrimer size-dependent change in the conformation of the Fc core. If the dendrimer size increases beyond a threshold, inter-peptide H-bonding holding the system in the 1,2′-conformation should get sufficiently destabilized to allow changes in the conformation of the Fc core. This in turn should be noticeable in the Fc region of the circular dichroism spectrum of the dendrimers. Here we report the synthesis, characterization, and properties of disubstituted Fc−peptide Glu dendrimers from G1 to G6.

Experimental Section

General Materials. All syntheses were carried out in air unless otherwise indicated. CH_2Cl_2, THF, and $CHCl_3$ (BDH; ACS grade) used for synthesis, FT-IR, and electrochemistry were dried (CaH_2) and distilled under N_2 prior to use. Acetone, EtOAc, CH_3CN, MeOH, diethyl ether (BDH; ACS grade), hexanes (Fischer; HPLC grade), $CHCl_3$, and CH_2Cl_2 used for the purpose of purification were used as received. $CDCl_3$ and CD_3CN (Aldrich) were dried by and stored over molecular sieves (8−12 mesh; 4 Å effective pore size; Fisher) before use. Ferrocene dicarboxylic acid (Aldrich), EDC, HOBt, H-Glu-OEtHCl (Aldrich), Na_2SO_4, $NaHCO_3$ (VWR), and Boc-GluOH were used as received. Et_3N (BDH; ACS grade) used in Fc−amino acid couplings was dried by molecular sieves when used in stoichiometric quantities. For column chromatography, a column with a width of 2.7 cm (i.d.) and a length of 45 cm was packed 18−22 cm high with 230−400 mesh silica gel (VWR). For TLC, aluminum plates coated with silica gel 60 F_{254} (EM Science) were used.

General Peptide Coupling by the Carbodiimide Method. A slurry composed of the carboxylic acid-terminated compounds Fc-$[COOH]_2$, and Boc-GluOH in dry CH_2Cl_2 (may contain 5% THF) and 2.2 equiv of HOBt and EDC added in succession was formed in a reaction vessel at controlled temperature in ice at 0 °C. In a separate reaction vessel, the coupling free N-terminal amino acid/

* Corresponding author: Fax +1-306-966-4730; Tel +1-306-966-4660; e-mail kraatz@skyway.usask.ca.

10.1021/ma060525x CCC: $33.50
Published on Web 07/22/2006

peptide/dendrimer (may be obtained by in situ TFA deprotection of the Boc group) was dissolved in a minimal amount of dry CH_2Cl_2 and made basic with an equivalent amount of Et_3N. Mixing of the two reaction mixture leads to a clear solution which is stirred continuously for 18−120 h. The work-up involves the use of standard aqueous procedure involving the subsequent use of saturated $NaHCO_3$ solution, 10% citric acid solution, and saturated $NaHCO_3$ solution followed by distilled water, collecting, and drying of the organic layer to obtain the crude product. Saturated NaCl was used in situations were emulsions are formed.

General Boc Deprotection with TFA. For the preparation of Boc-protected higher generations and Fc-functionalized compounds, Boc protecting groups of precursor compounds were deprotected with TFA in DCM (1:1 v/v ratio) usually for 2 h. The mixture was stirred initially in ice and then at room temperature. The reaction mixture is then pumped to dryness and finally neutralized with Et_3N in dry CH_2Cl_2 to afford the free N-terminal peptide for amide coupling.

Synthesis of G1: Synthesis of Fc-[Glu-OEt]$_2$ was carried out by coupling Fc-[COOH]$_2$ (0.9 g, 3.0 mmol) in CH_2Cl_2/THF (19:1) (dry) to H-Glu-(OEt)$_2$-HCl (3.0 g) in dry CH_2Cl_2 (50 mL) for 18 h. Purification of the crude product involved column chromatography using hexane/EtOAc/$CHCl_3$ 4:3:3, $R_f = 0.3$. Yield: 0.5 g, 63%. HR-MS (FAB): calculated for $C_{30}H_{40}N_2O_{10}Fe = 634.2032$ $[M + 1]^+$; found: 635.2927. ^{1}H NMR (δ in ppm of $CDCl_3$): 8.30 (2H, d, $J = 8.1$ Hz, NH-Glu), 4.88 (2H, s, CH−Cp), 4.82 (2H, s, CH−Cp), 4.42 (2H, s, CH−Cp), 4.39 (2H, s, CH−Cp), 4.35 (1H, m, CH$^\alpha$−Glu), 4.12 (2H, m, CH_2−O), 4.07 (2H, q, $J = 7.2$ Hz, CH_2−O), 2.45 (2H, t, $J = 7.3$ Hz, CH_2−Glu), 2.09 (1H, m, CH_2−Glu), 1.96 (1H, m, CH_2−Glu), 1.21 (3H, t, $J = 7.2$ Hz, CH_3 ester), 1.17 (3H, t, $J = 7.3$ Hz, CH_3 ester). ^{13}C{^{1}H} NMR (δ in ppm DMSO-d_6): 173.1, 172.9, 170.0 (C═O), 77.5, 73.0, 72.8, 71.0, 70.3 (Cp), 61.5, 60.8 (O−CH_2 ester), 52.3 (C$^\alpha$, Glu), 31.0 (CH_2 Glu), 26.5 (CH_2 Glu), 14.9 (CH_3 ester). IR (KBr, cm^{-1}): 3303 (NH amide A), 3099 (s, CH of Cp),1733 (s, C═O ester), 1633 (s, amide I), 1545 (s, amide II). UV−vis (CH_3OH, λ_{max} in nm, ϵ in cm^{-1} M^{-1}): 440 (345).

Synthesis of Boc-G2OEt: The compound was obtained from the coupling of Boc-GluOH (1.8 g, 7.4 mmol) in CH_2Cl_2 (50 mL) with H-Glu-OEt·HCl (4.50 g, 18.0 mmol) dissolved in CH_2Cl_2 (10 mL).The reaction was stirred continuously for 36 h. The crude product was purified by column chromatography ($R_f = 0.4$; 10% MeOH in $CHCl_3$). Yield = 3.7 g, 73%. ^{1}H NMR ($CDCl_3$, δ in ppm): 7.88 (1H, d, $J = 8.6$ Hz, NH), 7.65 (1H, d, $J = 8.3$ Hz, NH), 5.02 (1H, d, $J = 7.2$ Hz, NH), 4.72 (1H, m, H$^\alpha$−Glu), 4.65 (1H, m, H$^\alpha$−Glu), 4.13 (8H, m, OCH_2), 3.96 (1H, m, H$^\alpha$−Glu), 2.45 (4H, m, CH_2 of Glu), 2.33 (6H, m, CH_2 of Glu), 1.87 (4H, m, CH_2 of Glu), 1.12 (3H, t, CH_3), 1.42 (9H, s, CH_3 of Boc). ^{13}C{^{1}H} NMR (δ in ppm, $CDCl_3$): 173.0, 172.9, 172.8, 172.6, 172.3 (C═O), 156.1 (C═O Boc), 79.2 (C−O Boc), 61.3, 60.7 (C$^\alpha$ of Glu), 55.7, 55.6, 53.9 (CH_2−O ester), 32.4, 30.5, 26.0, 26.0, (CH_2 Glu), 25.9, 13.2 (CH_3).

Synthesis of G2: The compound was synthesized by coupling of Fc-[COOH]$_2$ (0.07 g, 0.3 mmol) in CH_2Cl_2 (200 mL) to the product of TFA deprotected Boc-G2OEt (3.0 g, 18.2 mmol) dissolved in CH_2Cl_2 (100 mL) at room temperature for 48 h. Crude product was purified by column chromatography ($R_f = 0.7$; 5% MeOH in $CHCl_3$), giving an orange solid. Yield: 1.2 g, 56%. HR-MS (FAB): calculated for $C_{58}H_{85}N_6O_{22}Fe$: 1276.4895 $[M + 1]^+$; found 1276.6293. ^{1}H NMR ($CDCl_3$, δ in ppm): 8.25 (2H, d, $J = 9.3$ Hz, NH), 8.20 (2H, d, $J = 7.3$ Hz, NH), 7.79 (2H, d, $J = 8.9$ Hz, NH), 4.92 (2H, m, CH$^\alpha$−Glu), 4.83, 4.60,4.51, 4.25 (8H, Cp), 4.67 (2H, m, H$^\alpha$−Glu), 4.35 (2H, m, H$^\alpha$−Glu), 4.23 (8H, m, OCH_2), 4.14 (8H, m, OCH_2), 2.76 (1H, m, CH$^\alpha$−Glu), 2.48 (3H, m, CH$^\alpha$−Glu), 2.37 (2H, m, CH$^\alpha$−Glu), 2.24 (4H, m, CH$^\alpha$−Glu), 1.98(2H, m, CH$^\alpha$−Glu), 1.29 (12H, m, CH_3). ^{13}C{^{1}H} NMR (δ in ppm, $CDCl_3$): 179.7, 174.3, 174.0, 173.2, 173.0, 172.9, 172.4, 172.3 (C═O), 75.6, 71.6, 71.3,70.1, 69.6 (Cp), 62.6, 62.5, 61.1, 61.0 (CH_2−O), 52.9, 52.8, 52.1 (C$^\alpha$ of Glu), 32.7, 31.1, 30.9, 29.5, 27.0, 25.3 (CH_2 of Glu), 14.6, 14.5 (CH_3). IR (KBr, cm^{-1}): 3455, 3303 (NH amide A), 3094 (s, CH of Cp), 1737 (s, C═O ester), 1661 (s, amide I), 1540 (s, amide II). UV−vis ($CHCl_3$, λ_{max} in nm, ϵ in cm^{-1} M^{-1}): 440 (413).

Synthesis of Boc-G3OEt: Boc-G3OEt was synthesized by coupling Boc-GluOH (0.25 mg, 1.0 mmol) in 50 mL to the product of TFA deprotected Boc-G2OEt (1.70 g, 2.4 mmol) in CH_2Cl_2 (20 mL). After stirring for 36 h, the crude product was purified by column chromatography ($R_f = 0.4$; 10% MeOH in $CHCl_3$). Yield: 0.80 g, 64%. ^{1}H NMR ($CDCl_3$, δ in ppm): 8.55 (1H, d, $J = 8.6$ Hz, NH), 8.28 (2H, d, $J = 8.3$ Hz, NH), 7.79 (1H, d, $J = 7.9$ Hz, NH), 7.54 (1H, d, $J = 7.6$ Hz, NH), 4.95 (1H, d, $J = 7.1$ Hz, NH), 4.84 (1H, m, CH$^\alpha$−Glu), 4.68 (1H, m, CH$^\alpha$−Glu), 4.23 (8H, m, OCH_2), 4.13 (8H, m, OCH_2), 3.96 (1H, m, CH$^\alpha$−Glu), 2.46 (14H, m, CH_2 of Glu), 2.27 (14H, m, CH_2 of Glu), 1.29 (24H, m, CH_3), 1.46 (9H, s, CH_3 of Boc). ^{13}C{^{1}H} NMR (δ in ppm, $CDCl_3$): 174.5, 174.4, 174.19, 173.0, 172.8, 172.7 (C═O), 155.4 (C═O of Boc), 62.7, 62.6, 62.5, 61.1, 60.9, 60.5 (OCH_2), 53.8, 53.5, 52.1, 51.9 (C$^\alpha$ of Glu), 32.5, 31.7, 31.2, 30.8, 30.5, (CH_2 of Glu), 27.7 (CH_3 of Boc), 14.6 (CH_3).

Synthesis of G3: The synthesis of **G3** was achieved by coupling of Fc-[COOH]$_2$ (0.27 g, 0.93 mmol) in CH_2Cl_2 (200 mL) to the product of TFA deprotected Boc-G3OEt (3.0 g, 13 mmol) dissolved in CH_2Cl_2 (100 mL) at room temperature for 48 h. The product was purified by column chromatography ($R_f = 0.7$; 7% MeOH in $CHCl_3$), giving an orange solid. Yield = 0.65 g, 42%. HR-MS (FAB): calculated for $C_{114}H_{173}N_{14}O_{46}Fe = 2532.0649$ $[M + 1]^+$; found = 2533.1574. ^{1}H NMR ($CHCl_3$, δ in ppm): 8.64 (1H, d, $J = 6.8$ Hz, NH), 8.20 (1H, d, $J = 8.5$ Hz, NH), 8.15 (2H, d, $J = 6.5$ Hz, NH), 8.09 (2H, d, $J = 9.2$ Hz, NH), 8.00 (2H, d, $J = 7.3$ Hz, NH), 7.88 (1H, d, $J = 8.6$ Hz, NH), 7.74 (2H, d, $J = 8.9$ Hz, NH), 7.63 (2H, d, $J = 8.5$ Hz, NH), 7.44 (1H, d, $J = 8.5$ Hz, NH), 7.03 (1H, d, $J = 7.1$ Hz, NH), 4.85 (2H, m, H$^\alpha$−Glu), 4.74 (1H, s, H Cp), 4.70 (1H, m, CH$^\alpha$−Glu), 4.57 (7H, m, CH$^\alpha$−Glu and H of Cp), 4.51 (1H, s, H of Cp), 4.30 (3H, m, H$^\alpha$−Glu), 4.25 (1H, s, H of Cp), 4.14 (34H, m, OCH_2), 3.92 (5H, m, H$^\alpha$ Glu), 3.70 (1H, m, H$^\alpha$−Glu), 2.54 (2H, m, CH_2 of Glu), 2.38 (22H, m, CH_2 of Glu), 2.19 (23H, m, CH_2 of Glu), 1.87 (19H, m, CH_2 of Glu), 1.22, 1.17, 1.04 (54H, m, CH_3). ^{13}C{^{1}H} NMR (δ in ppm, $CHCl_3$): 174.4, 174.3, 173.3, 173.2, 173.1, 173.0, 172.8, (C═O), 72.8, 72.3, 71.7, 70.3 (Cp), 68.5 (C^m), 62.7, 62.5, 61.0, 60.7 (OCH_2) 53.5, 53.2, 52.2, 52.1, 51.9 (CH$^\alpha$ Glu), 32.3, 31.1, 30.8, 30.7, 27.4, 27.3, 27.1, 26.9 (CH_2 Glu), 14.6, 14.5 (CH_3). IR (KBr, cm^{-1}): 3303 (s, amide A), 3080 (s, CH of Cp), 1736 (s, C═O ester), 1643 (s, amide I), 1545 (s, amide II). UV−vis ($CHCl_3$, λ_{max} in nm, ϵ in cm^{-1} M^{-1}): 444 (394).

Synthesis of Boc-G4OEt: Boc-G4OEt was synthesized by coupling Boc-GluOH (2.50 g, 10.0 mmol) in CH_2Cl_2 (200 mL) to the product of TFA deprotected Boc-G3OEt (2.10 g, 9.0 mmol) dissolved in CH_2Cl_2 (100 mL). After further stirring 48 h, the reaction was worked up as described above. Additionally, saturated NaCl was used to break up emulsion formed during the workup stages. The crude product was purified by column chromatography ($R_f = 0.4$; 10% MeOH in $CHCl_3$). Yield = 2.30 g, 36%. ^{1}H NMR ($CDCl_3$, δ in ppm): 8.2−7.37 (10H, m, NH,), 7.01 (3H, m, NH), 5.7(1H, m, NH), 5.41 (1H, m, NH), 4.76−4.48 (1H, m, CH$^\alpha$−Glu), 4.21−4.13 (8H, m, CH_2), 2.45 (4H, m, CH_2 of Glu), 2.21 (6H, m, CH_2 of Glu), 1.96 (4H, m, CH_2 of Glu), 1.42 (9H, s, CH_3 of Boc), 1.27 (48H, m, CH_3 of ester). ^{13}C{^{1}H} NMR (δ in ppm, $CDCl_3$): 173.9, 173.0 (C═O), 156.2 (C═O Boc), 78.9 (C−O Boc), 62.6, 62.4, 61.1 (CH_2−O ester), 52.9, 52.2 (C$^\alpha$ of Glu), 32.3, 31.0, 30.8, 30.1, 27.2 (CH_2 Glu), 14.5 (CH_3 of Et group).

Synthesis of G4: The compound was synthesized by coupling of Fc-[COOH]$_2$ (0.33 g, 1.2 mmol) in CH_2Cl_2 (300 mL) to the product of TFA deprotected Boc-G4OEt (3.5 g, 11.6 mmol) dissolved in CH_2Cl_2 (100 mL) at room temperature for 4 days. The crude product is purified by column chromatography ($R_f = 0.4$; 10% MeOH in $CHCl_3$), giving an orange solid. Yield = 0.80 g, 38%. HR-MS: calculated for $C_{226}H_{349}N_{30}O_{94}Fe = 5045.2473$; found = 5045.3014. ^{1}H NMR ($CDCl_3$, δ in ppm): 8.77 (1H, d, $J = 6.7$ Hz, NH), 8.64 (1H, d, $J = 6.6$ Hz, NH), 8.29 (2H, d, $J = 6.8$ Hz,NH), 8.20 (3H, m, NH), 8.09 (3H, m, NH), 8.00 (3H, m, NH), 7.91 (1H, d, $J = 6.9$ Hz, NH), 7.80 (4H, m, NH), 7.63 (6H, m,

NH), 7.30 (1H, d, $J = 7.6$ Hz, NH), 6.98 (2H, d, $J = 6.6$ Hz, NH), 6.86 (2H, d, $J = 7.1$ Hz, NH), 6.44 (2H, d, $J = 8.4$ Hz, NH), 6.38 (3H, d, $J = 7.0$ Hz, NH), 6.10 (1H, d, $J = 7.4$ Hz, NH), 4.70, 4.54, 4.49, 4.24 (Cp), 4.24−4.16 (56H, m, OCH_2), 4.89−3.32 (30H, m, H^{α} Glu), 2.63, 2.46, 2.24, 1.98 (100H, m, CH_2 of Glu), 1.30, 1.26 (92H, m, CH_3). $^{13}C\{^1H\}$ NMR (δ in ppm, $CHCl_3$): 179.0, 174.4, 174.5, 174.0, 173.0, 173.9, 173.3, 173.0, 172.3, 171.8, 170.0, 169.6 (C═O), 72.2, 71.2, 70.3 (Cp), 62.6, 62.5, 61.1, 61.0, 60.9 (OCH_2) 53.7, 53.4, 52.1, 52.0, 51.9, 51.5, 49.6 (CH^{α}−Glu), 34.29, 32.4, 31.0, 30.8, 30.1, 29.7, 28.8, 28.7, 27.1, 27.0, 26.0, 25.9, 25.3 (CH_2−Glu), 14.5, 13.4 (CH_3). IR (KBr, cm^{-1}): 3298 (w, amide A), 3084 (s, CH of Cp), 1737 (s, C═O ester), 1640 (s, amide I), 1545 (s, amide II). UV−vis ($CHCl_3$, λ_{max} in nm, ϵ in cm^{-1} M^{-1}): 446 (292).

Synthesis of Boc-G5OEt: Boc-G5OEt was synthesized by coupling Boc-GluOH (0.25 g, 1.0 mmol) in CH_2Cl_2 (200 mL) to the product of an in situ TFA deprotected Boc-G4OEt (1.70 g, 2.4 mmol) dissolved in CH_2Cl_2 (50 mL). After further stirring 48 h, the reaction was worked up as described above. After evaporation of the organic phase, the crude product is purified by column chromatography ($R_f = 0.4$; 10% MeOH in $CHCl_3$). Yield = 1.2 g, 33%. ^1H NMR ($CDCl_3$, δ in ppm): 8.18−7.28 (31H, NH), 4.84 (1H, m, CH^{α}−Glu), 4.80−4.58 (31H, m, CH^{α}−Glu), 4.13−4.05 (64H, m, OCH_2), 2.47−1.8 (124H, m, CH_2 of Glu), 1.42 (9H, s, CH_3 of Boc), 1.21−1.17 (96H, m, CH_3). $^{13}C\{^1H\}$ NMR (δ in ppm, $CDCl_3$): 174.2, 174.1, 173.9, 173.8, 173.4, 173.2, 172.7, 172.6, 172.5, 172.3, (C═O), 156.3 (C═O Boc), 78.6 (C−O Boc), 62.5, 62.2, 62.1, 60.5, 60.6, 60.4 (OCH_2) 53.4, 53.3, 53.0, 51.7, 51.6, 51.5, 51.4 (CH^{α}−Glu), 33.7, 32.0, 31.9, 30.7, 27.4, 27.2, 27.0, 26.8, 26.5, 26.2 (CH_2−Glu), 14.4, 14.8 (CH_3).

Synthesis of G5: The compound was synthesized by coupling of Fc-$[COOH]_2$ (28 mg, 0.10 mmol) in CH_2Cl_2 (300 mL) to the product of an in situ TFA deprotected Boc-G5OEt (1 g, 0.27 mmol) dissolved in CH_2Cl_2 (100 mL) at room temperature for 4 days. The product was purified by column chromatography ($R_f = 0.3$; 7% MeOH in $CHCl_3$). The light yellow product was obtained at a yield of 0.70 g, 42%. HR-MS: calculated for $C_{450}H_{701}N_{62}O_{126}Fe$ = 9048.9371 (experimental value could not be obtained). ^1H NMR ($CHCl_3$, δ in ppm): 8.32−6.84 (62H, NH), 4.87−4.27 and 4.13−4.04 (128H, m, OCH_2 overlapping with Cp H), 3.88−3.67, 3.31−3.27 (124H, m, H^{α}−Glu), 2.43−1.88 (248H, m, CH_2 of Glu), 1.22−1.17 (194H, m, CH_3). $^{13}C\{^1H\}$ NMR (δ in ppm, $CHCl_3$): 174.0, 173.3, 172.6, 172.4, 172.2, (C═O), 74.6, 71.5, 70.1 (Cp), 62.3, 62.1, 60.6, 60.4 (OCH_2), 51.8, 51.7 (CH^{α}−Glu), 30.7, 30.6, 27.2, 26.8, 26.5 (CH_2−Glu), 14.0, (CH_3). IR (KBr, cm^{-1}): 3292 (s, amide A), 3075 (s, CH of Cp), 1737 (s, C═O ester), 1640 (s, amide I), 1545 (s, amide II). UV−vis ($CHCl_3$, λ_{max} in nm, ϵ in cm^{-1} M^{-1}): 432 (151).

Synthesis of Boc-G6OEt: Boc-G6OEt was synthesized by coupling Boc-GluOH (0.04 g, 0.15 mmol) in CH_2Cl_2 (100 mL) to the product of an in situ TFA deprotected Boc-G5OEt (1.3 g, 0.35 mmol) dissolved in CH_2Cl_2 (50 mL). After stirring for 6 days, the reaction solution was subjected to the aqueous work-up as described. The crude product is purified by column chromatography (R_f = 0.4; 10% MeOH in $CHCl_3$). Yield = 1.3 g, 50%. ^1H NMR ($CDCl_3$, δ in ppm): 8.64−7.27 (63H, m, NH), 4.87−4.66 (63H, m, CH^{α}−Glu), 4.22−4.10 (128H, m, OCH_2), 2.52−1.93 (256H, m, CH_2 of Glu), 1.32 (9H, s, CH_3 of Boc), 1.29−1.22 (192H, m, CH_3). $^{13}C\{^1H\}$ NMR (δ in ppm, $CDCl_3$): 174.3, 174.1, 174.0, 173.9, 173.8, 173.4, 173.0, 172.7, 172.6, 172.5, 172.4, 172.3, (C═O), 156.1 (C═O Boc), 78.8 (C−O Boc), 62.3, 62.2, 62.0, 60.5, 60.6, 60.4 (OCH_2) 53.4, 53.3, 53.0, 51.7, 51.6, 51.5, 51.4 (CH^{α}−Glu), 33.2, 32.0, 31.9, 30.7, 30.2, 30.0, 27.4, 27.3, 27.2, 27.0, 26.8, 26.5, 26.4 (CH_2 Glu), 14.2, 14.1,14.0 (CH_3).

Synthesis of G6: The synthesis of the compound was achieved by coupling of Fc-$[COOH]_2$ (16.8 mg, 0.06 mmol) in CH_2Cl_2 (300 mL) to the product of TFA deprotected Boc-G6OEt (1.02 g, 0.13 mM) in CH_2Cl_2 (200 mL) for 5 days. The product was purified by column chromatography ($R_f = 0.3$; 7% MeOH in $CHCl_3$) giving an light yellow solid. Yield = 0.35 g, 24%. HR-MS: calculated for $C_{898}H_{1405}N_{126}O_{254}Fe$ = 15134.4457 $[M + 1]^+$ (experimental value was not obtained by MALDI, ESI, and FAB). ^1H NMR ($CDCl_3$, δ in ppm): 8.98−7.68 (125H, NH), 4.89−4.26 (H of Cp overlaps with other peaks), 4.19−4.10 (256H, m, OCH_2), 3.72−3.62 (126H, m, CH^{α}−Glu), 2.52−1.62 (512H, m, CH_2 of Glu), 1.27−1.22 (384H, m, CH_3). $^{13}C\{^1H\}$ NMR (δ in ppm, $CDCl_3$): 179.1, 174.3, 173.7, 173.4, 173.1, 173.0, 172.9, 172.8, 172.2 (C═O), 62.7, 71.1, 69.9 (Cp), 62.5, 62.2, 61.0, 60.9, 60.8 (OCH_2), 53.3−51.1 (CH^{α}−Glu), 33.3−25.9 (CH_2−Glu), 14.5 (CH_3). IR (KBr, cm^{-1}): 3286, (s, amide A), 3070 (s, CH of Cp), 1735 (s, C═O ester), 1643 (s, amide I), 1540 (s, amide II). UV−vis: very weak.

NMR Measurements. NMR spectra were recorded on a Bruker Avance 500 spectrometer operating at 500 MHz (^1H) and 125 MHz ($^{13}C\{^1H\}$). Peak positions in both ^1H and ^{13}C spectra are reported in ppm relative to TMS. ^1H NMR spectra of Fc−peptides are referenced to the CH_2Cl_2 resonance (δ 5.32) of an external standard ($CDCl_3/CH_2Cl_2$). ^1H spectra of all other compounds are referenced to the residual $CHCl_3$ signal. All $^{13}C\{^1H\}$ spectra are referenced to the $CDCl_3$ signal at δ 77.23. Other NMR measurements (determination of H-bonding by DMSO addition and determination of diffusion coefficients by PGSE NMR) were carried out as reported before.[10]

UV−Vis Spectroscopy. Measurements of absorption spectra were carried out on a CARY 500 Scan-UV/vis NIR double-beam spectrophotometer. The UV−vis absorption spectra were recorded in the wavelength range of 300−600 nm in the absorbance mode using quartz cuvettes of 1 mm path length. All measurements were done in MeOH in concentration ranges of 1.0−6.0 mM of compounds with background subtraction of MeOH.

CD Spectroscopy. CD spectroscopic measurements were carried out on a π*-180 spectrometer, using HPLC grade MeOH and quartz cuvettes with a 1.0 mm path length. Mean molar ellipticities were calculated according to eq 1, where $[\theta]_{obs}$ is the observed ellipticity measured in degrees, l is the path length of the cell in centimeters, and c is the molar concentration of the peptide.

$$[\theta] = \frac{[\theta]_{obs}}{10lc} \tag{1}$$

IR Spectroscopy. IR experiments were carried out on Bio-Rad FTS-40 Fourier transform spectrometer. IR spectra were acquired as a KBr disk for the general characterization. For study of hydrogen bonding in ester compounds, IR spectra were acquired in solutions of 1.0−50.0 mM compounds in $CHCl_3$ using liquid IR cell NaCl windows with path length 0.025 mm. In all cases background spectra were collected and applied to sample spectra. Spectra were recorded at a temperature of 22 ± 5 °C and a resolution of 4 cm^{-1}.

Solution Electrochemical Measurements. All electrochemical experiments were carried out at room temperature (23 ± 1 °C) on a CV-50W voltammetric analyzer (BAS) using a glassy carbon as working electrode, a Pt wire as counter electrode, and a Ag/AgCl (3.0 M NaCl, BAS) as a reference electrode, as described before.[10]

Molecular Modeling. Geometry optimization of the 3D conformational structure of the full ferrocene dendrimers was performed in a vacuum by a molecular mechanics method (Merck Molecular Force Field) in Spartan'05 (Wave Function Inc., Irvine, CA). The input data were derived from the builder routine in the package. In these calculations, the individual cyclopentadienyl rings and the Fe of the core were forced into a sandwich geometry using the constrain dihedral option to prevent deformations. The three-dimensional shape of all compounds has been simulated by energy minimization of the molecules. Solvent effects were excluded in the calculations. All models are presented as space-filled representations. For the calculation of the torsion angles within the ferrocene unit and for their visualization, the glutamic acid dendrimers were removed after energy minimization on the ferrocene dendrimers.

Results and Discussion

Synthesis and Characterization. The synthesis of disubstituted Fc−peptide dendrimers is summarized in Scheme 1. Coupling of Fc-$[COOH]_2$ with 2 equiv of H-Glu(OEt)-OEt·HCl

Scheme 1. Schematic Representation of the Synthesis of Disubstituted Fc−Peptide Dendrimers[a]

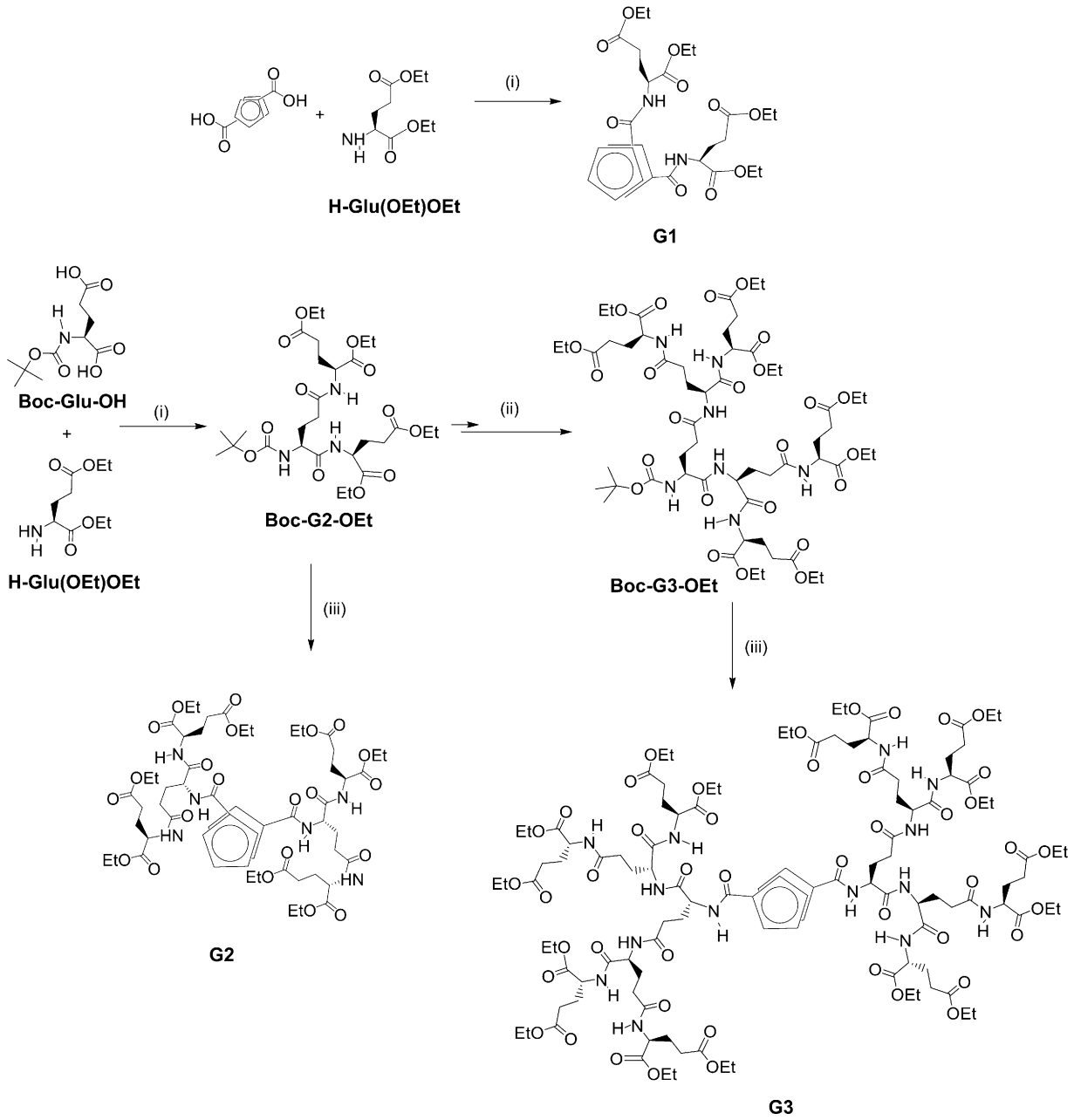

[a] (i) Coupling of Boc-GluOH and H-Glu(OEt)-OEt·HCl in the presence of HOBt/EDC/Et_3H in CH_2Cl_2 gives the Boc-G2. (ii) Sequential Boc deprotection with TFA/CH2Cl_2 followed by coupling with Boc-GluOH yielding Boc-G3. (iii) Boc deprotection with TFA/CH2Cl_2 followed by coupling the Fc-$[COOH]_2$ in the presence HOBt/EDC/Et_3N in CH2Cl_2 gives the Fc−peptide dendrimers **G2** and **G3**. Sequential amide coupling, TFA deprotection, and coupling to Fc-$[COOH]_2$ yields higher generations.

results in the formation of the first generation **G1**. For the higher generations **G2**−**G6**, a convergent strategy was adopted.[15,16] This involved the synthesis of the Boc-protected peptide dendrimers derivatives (Boc-G2 to Boc-G6), followed by coupling to Fc-$[COOH]_2$ to generate the disubstituted Fc dendrimers **G2**−**G6**.

Despite the potential steric inhibition of the amino group in Boc-G6, the reaction with Fc-$[COOH]_2$ results in the formation of **G6** in relatively good yields (Table 1). It is speculated that this is due to the enhanced solubility of Boc-G6 in dichloromethane, which may allow better penetration into the center of dendrimer and enable a more facile reaction with the Fc synthon.

The dendrimers **G1**−**G6** are represented diagrammatically in Scheme 2 showing geometric ($4^{G(n)}$) increase in the number of terminal ester (OEt) groups with increasing generations (G(*n*) where $n = 1-6$). All dendrimers were obtained as yellow to orange solids after purification by column chromatography on silica gel and were investigated spectroscopically by NMR, UV−vis, and ESI-MS. Some physical properties of **G1**−**G6** are summarized in Table 1. Although for **G1**−**G4**, molecular

Table 1. Some Properties of Disubstituted Fc−Peptide Dendrimers G1−G6

compd	NH's	OEt groups	% yield	C−H of Cp	calcd molecular mass	experimentally determined $[M + 1]^+$
G1	2	4	63	3099	634.2032	635.1927
G2	6	8	56	3094	1276.4895	1277.0293
G3	14	16	42	3080	2532.0649	2533.1574
G4	30	32	38	3084	5045.2473	5045.3014
G5	62	64	42	3075	9048.9371	nd
G6	126	128	24	3070	15134.4457	nd

Scheme 2. Schematic Representation of Disubstituted Fc−Peptide Dendrimers Fc−[G1OEt]$_2$, Fc−[G2OEt]$_2$, Fc−[G3OEt]$_2$, Fc−[G4OEt]$_2$, Fc−[G5OEt]$_2$, and Fc−[G6OEt]$_2$

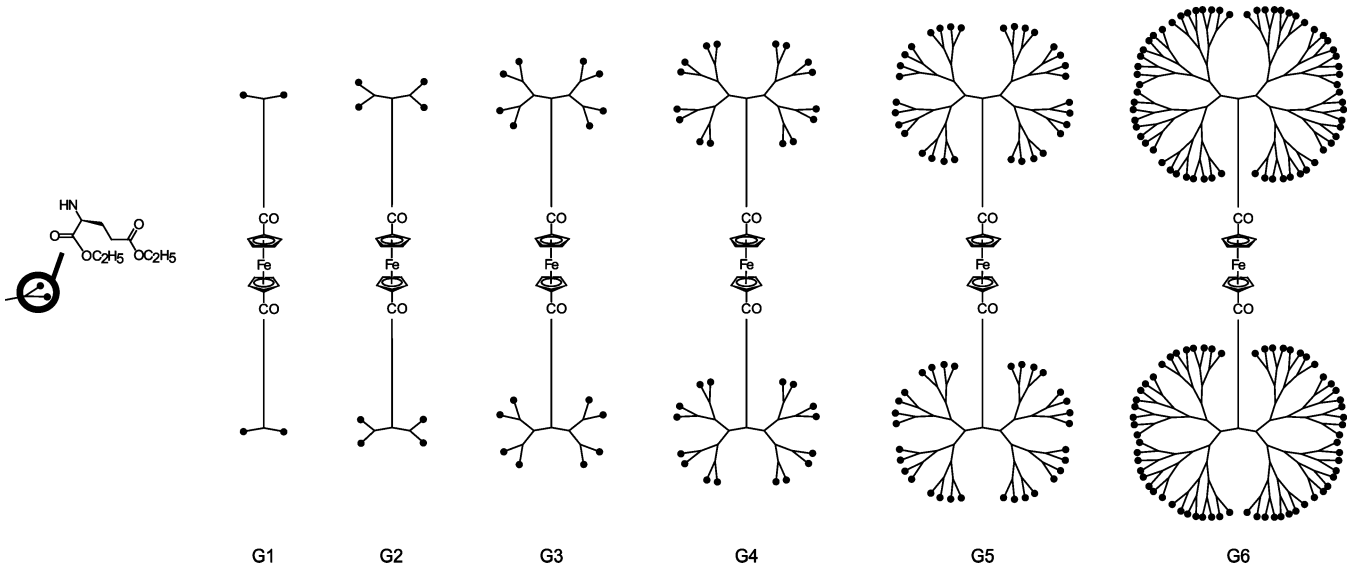

ions were observed, we did not succeed in observing them for the higher generations **G5** and **G6**. Instead, only fragmentation was observed by ESI, FAB, and even MALDI. In the IR, each dendrimer exhibits a distinct C−H stretching vibration. As we showed before for monosubstituted Fc−glytamic acid dendrimers, the C−H stretching vibration is shifting to lower wavenumbers upon an increase in dendrimer generation.[10]

The algebraic increase in the number of NH's and carbonyl groups with increasing generation demonstrates the successful synthesis of the disubstituted Fc−peptide dendrimers. For example, the ^{1}H NMR for **G1**−**G6** exhibits 2, 6, 14, 30, 62, and 126 amide NHs, respectively. In **G4** to **G6** the amide peaks are overlapping, preventing the assignment of the individual signals. The Fc group in disubstituted compounds **G1** to **G4** exhibit signals characteristic of disubstituted Fc compounds showing four or two broad singlets Cp-H at δ 4.91−4.23.[9,17] The Hs of the Cp groups of **G5** and **G6** overlap with α-H of the Glu-dendrimer and are generally less resolved.

While for the lower generations **G1** and **G2** (Figure 1) the amide signals are observed in a region of δ_{NH} 7.5−9.0, higher generations exhibit amide signals over a wider range δ_{NH} 6.0−9.0. This suggests that for higher generations some of the amides may not be involved in H-bonding, possibly due to steric hindrance. A wide range of amide NH shifts were also reported for other peptide and polyamide dendrimers.[18−20] In general, deshielding of the amide protons downfield of δ 7.5 is rationalized by the involvement of the amide NH in H-bonding. In poly(glutamic acid) dendrimers having adamantine cores, the amide NH resonance shifts to lower field with each successive generation.[18]

The UV−vis spectra of **G1**−**G6** recorded in methanol are shown in Figure 2. Each dendrimer with the exception of **G6** exhibits a broad characteristic absorbance for the Fc-based transition at λ_{max} = 450−435 nm for all generations except G5 and G6, where it is considerable reduced or absent under the experimental conditions of 1.0−6.0 mM. This may be associated with the total encapsulation of the Fc moiety in higher generations.

Chirality and Molecular Structure. Circular dichroism (CD) offers a means of assigning the helical chirality of the central Fc core in solution.[11−13,21] A positive Cotton effect indicates a 1,2′-conformation results in P-helicity of the central Fc group, while a negative Cotton effect is indicative of 1,5′-conformation and *M*-helicity. The CD spectra of dendrimers **G1**−**G6** in MeOH are shown in Figure 3. For the Fc-based transition, a positive Cotton effect is exhibited by all dendrimers except **G6**, indicating *P*-helicity of the central Fc core. Importantly, although the value of λ_{max} does not change, the molar ellipticity θ is changing as a function of the dendrimer size and decreases in intensity as the size of the dendrimer increases. No Fc-based CD band is observed for **G6**. We rationalize this observation

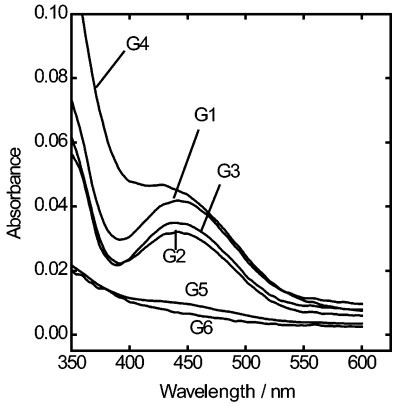

Figure 1. UV−vis of disubstituted Fc−peptide dendrimers (1.0 mM in MeOH).

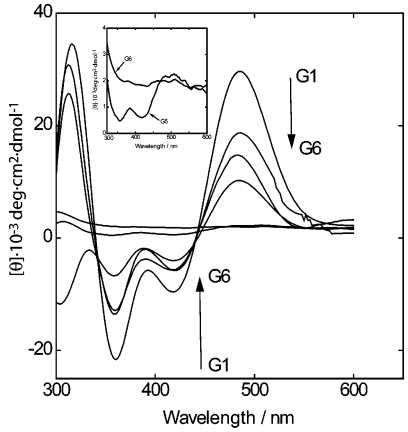

Figure 2. CD spectra of dendrimers **G1**−**G6** (inset expanded to show expanded region for **G5** and **G6** in the 300−600 nm region) in MeOH.

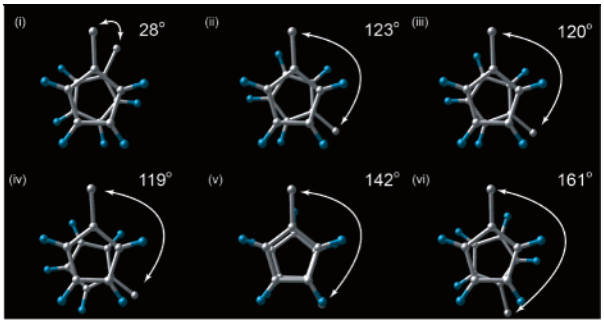

Figure 3. Conformation of the two Cp rings having glutamic acid dendrimer substituents, showing increasing torsion angles with increasing generation (i) **G1**, (ii) **G2**, (ii) **G3**, (iv) **G4**, (v) **G5**, and (vi) **G6**. The glutamic acid dendrimer substituents are omitted for clarity.

by conformational changes of the central Fc core. **G1** is a system that will display the typical 1,2′-substitution pattern of the Fc core and P-helicity. Rotation about the Cp(centroid)−Fe−Cp(centroid) axis is prevented by strong interstrand H-bonding. An increase of the dendrimer size increases the steric pressure and forces the system out of the 1,2′-conformation into other conformations that may result in a "racemization" of the Fc conformation. The changes for **G1**−**G4** are gradual, and the intensity of the Fc-based transition decreases. Importantly, variable temperature CD in the range of 20−45 °C did not show any changes in the intensity of the bands, suggesting that there is no equilibrium between conformations. Instead, we propose that equilibration into the lowest energy conformation takes place during the synthesis. There is a more dramatic decrease in the intensity for **G5**. It appears that the system is virtually achiral in Fc. For **G6** no CD signal was observed (see inset to Figure 3).

To evaluate potential structural changes taking place at the central Fc unit, we carried out energy minimizations using Spartan (see Figure 3). Our studies show that the torsion angle ω defined as the C(ipso)−Cp(centroid)−Cp(centroid)−C(ipso) between the two substituents on the Fc ring is small for **G1**, as would be expected for the system in a 1,2′-conformation. This value is slightly lower than the values reported for some strongly H-bonded disubstituted Fc−peptide systems, which generally adopt the "Herrick" conformation.[12,22,23] Values for ω between 26° and 41° were observed for 1,*n*′-bis(phosphino)ferrocene−metal complexes.[24] For **G2**−**G4**, ω is in the range of 120°, while for **G5** and **G6**, the angle increases dramatically to 142° and 161°, respectively. In the case of disubstituted Fc−peptides in which the peptides substituents cannot engage in interstrand H-bonding forcing a tight 1,2′-conformation, a noncongested approximate 1,3′-conformation is established. This "Xu" conformation has a torsion angle ω of −123°.[25] Since the structure of the Fc core appears to be strongly affected by the size of the dendrimer, we expected that this has significant effects on redox properties of the Fc core (vide infra).

From molecular modeling, the approximate dimensions of the disubstituted Fc−glutamic acid dendrimers were obtained. Figure 4 shows the energy-minimized structures adopted by the disubstituted Fc−peptide dendrimers **G1**−**G6** and their average diameters. The dendritic sheath begins by wrapping round the disubstituted Fc core and finally engulfs the whole Fc group in **G6**. It can be assumed that the changes in the molecular structure are facilitated by the backfolding of the flexible peptide branches. The backfolding process is enhanced by strong intramolecular H-bonding interactions within the peptide dendrimer. Phenylalanine-terminated dendrimers display a significant folding back of the dendrimers in the higher generations. As a result, the terminal groups may be distributed throughout the molecular volume.[26] Molecular dynamic simulations of alanine-terminated starburst dendrimers up to the seventh generation by Naylor indicated that the morphology of the dendrimers is dependent on the generational number and the presence of void spaces in the interior of the dendrimers.[27] A similar analysis by Lescanec and Muthkumar showed that backfolding of the chained was so extensive at higher generations that the primary dendrons could be found in the center of the dendrimers.[28]

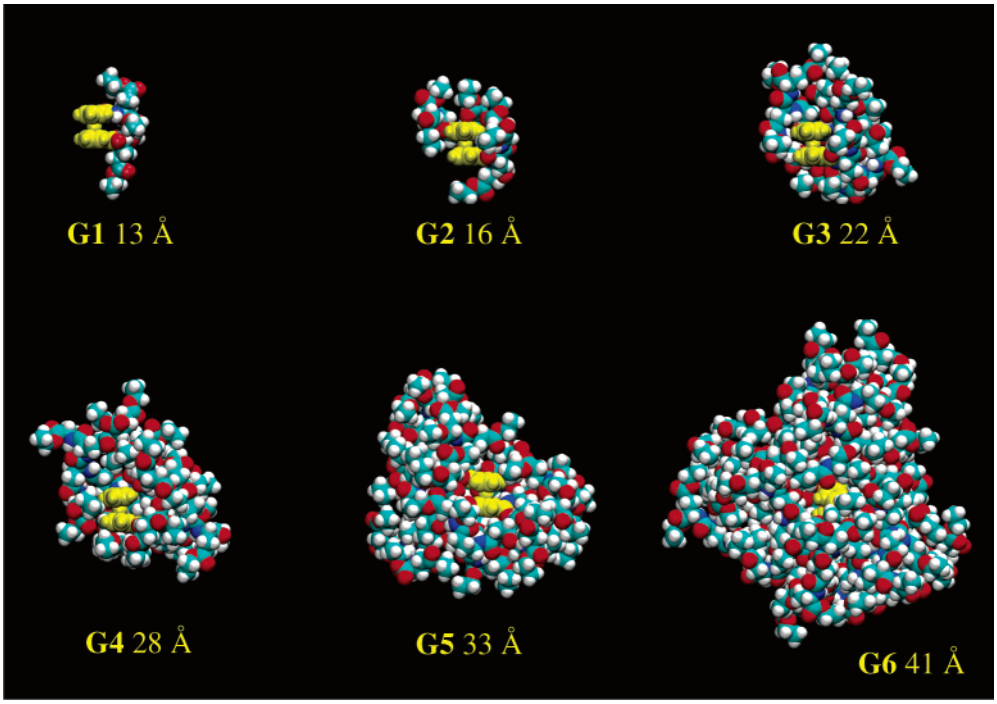

Figure 4. Molecular modeling of disubstituted Fc−glutamic acid dendrimers **G1** to **G6** with average diameters as shown. The degree of ferrocene encapsulation increases with higher generations. Fc (yellow), carbon (green), hydrogen (white), oxygen (red), nitrogen (blue).

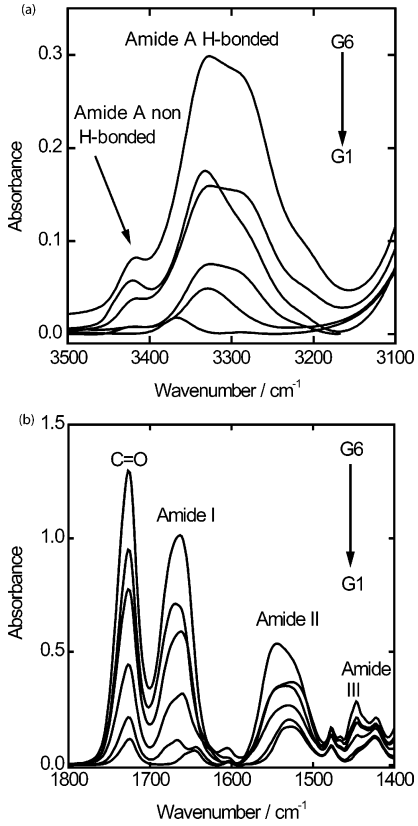

Figure 5. IR of the amide NH, carbonyl C═O, and amide I, II, III regions for disubstituted dendrimers **G1**−**G6**.

Table 2. Selected IR (cm^{-1}) Data for Fc−Peptide Dendrimers Taken in $CHCl_3$ Solution (2.0 mM)[a]

compd	NH	C═O	amide I	amide II	amide III
G1	3289, 3367	1717	1643	1529	1446, 1423
G2	3413, 3333	1723	1666, 1644	1529	1446, 1423
G3	3419, 3333	1729	1674, 1661	1529	1446, 1423
G4	3421, 3331	1726	1669	1529	1446, 1423
G5	3419, 3331	1729	1666	1534, 1522	1444, 1419
G6	3418, 3330	1723	1666	1540	1444, 1419

[a] Recorded at a resolution of 4 cm^{-1}. nd = experimental value could not be obtained. Yield in % represents single step from Boc to Fc compound. C−H of Cp from FT-IR by KBr.

Evaluation of Hydrogen Bonding. The next step in our study was the investigation of the H-bonding within the peptide dendrimer. The association of the amide groups in these dendrimers via H-bonding was investigated by means of IR and ^{1}H NMR spectroscopies in solution. Figure 5 shows a series of IR spectra for equimolar solutions of **G1**−**G6**. Table 2 summarizes the IR data. In all cases, two signals for the NH stretching vibration are observed between 3320 and 3440 cm^{-1}, which relates to the ratio of non-H-bonded and H-bonded amide NHs in these dendrimer systems.[29−31] The data suggest strongly H-bonded amides in all generations. Ala systems display IR signals attributable to the ester and the amide groups. The ester C═O group gives rise to signals between 1730 and 1717 cm^{-1}. Three amide bands were observed the systems: amide I band 1675−1643 cm^{-1} (C═O stretch), amide II band 1540−1530 cm^{-1} (C═ONH bend), and amide III band 1440−1423 cm^{-1} (NH in-plane bending). As expected, for equimolar concentrations, the intensity of these signals decreases with decreasing generation.

In solution, the amide I stretching vibrations is sensitive to H-bonding and to the environment of the amide groups and can be used to evaluate the secondary structure of peptides. Bands located at 1658−1650 cm^{-1} are associated with α-helical conformation while bands between 1640 and 1620 cm^{-1} and 1695−1670 cm^{-1} are indicative of parallel and antiparallel β-sheets, respectively.[32,33] It has also been generally suggested that bands in the region 1650−1640 cm^{-1} can be ascribed to random coil structures.[32,33]

Table 3. Solution IR Stretching Vibration and Absorbance Intensity for Amide NH H-Bonded and Non-H-Bonded Dendrimers at 2.0 mM in $CHCl_3$[a]

compd	amide A		ratio of H-bonded/ non-H-bonded[b]
	non H-bonded	H− bonded	
G1	not observed	3367 (0.017)	H-bonded
G2	3413 (0.009)	3333 (0.047)	5.2
G3	3419 (0.010)	3333 (0.078)	7.8
G4	3421 (0.058)	3331 (0.173)	3.0
G5	3419 (0.035)	3331 (0.157)	4.0
G6	3418 (0.082)	3330 (0.297)	3.6

[a] Recorded at a resolution of 4 cm^{-1}. [b] Intensity ratios derived from the most intense peaks in the deconvoluted spectra. Intensity of peaks is shown in parentheses. Ratios were reproducible to within 10%.

The values of amide I also show that increasing the size of the dendrimers beyond the first generation leads to changes in peptide conformation. It appears that the H-bonding for higher generations resembles that of a β-sheet or random coil structures, as would be probable for a globular peptide sheath. The amide II band has also been used to predict the presence of H-bonded and non-H-bonded amides in Fc−peptides.[17] Values in the range 1500−1510 cm^{-1} generally represent non-H-bonded amides while for H-bonded systems this value is shifted to the higher wavenumbers. The values obtained are in the H-bonded range 1540−1522 cm^{-1}, indicating H-bonding.

The ratio of peak intensities of H-bonded to non-H-bonded amide NH (A_{H-B}:$A_{non\ H-B}$) which relates to the proportion of molecules engaged in intramolecular H-bonding[34−36] is summarized in Table 3. **G1** shows an H-bonded amide A NH signal at 3367 cm^{-1} and a signal due to the amide B band at 3284 cm^{-1}. The amide B bands is attributed to Fermi resonance between the first overtone of the amide II and the NH stretching vibrations.[37−39] The amide B bands become more apparent at higher generations (Figure 6). The position of the amide A and B bands shifts on going from **G1** to **G6**, suggesting an increase in overall H-bonded character with increasing generations. In addition, on increasing the size of the dendrimers a non-H-bonded component becomes apparent in the 3420 cm^{-1} region for **G2**−**G6**.

The fact that the relative non-H-bonded character also increased with increasing generations is indicative that additional generations create potentially "loose" terminal amides which are less H-bonded. All amide NH for **G1** and **G2** are H-bonded, giving rise to signals in the ^{1}H NMR spectra in the region of δ 9.0−7.3. With increasing generation, the number of non-H-bonded signals upfield of δ 7.5 increases. For **G3**−**G6**, some amides NHs are observed in the region of δ 6.0−7.2 and are clearly not H-bonded.

Addition of a H-bond-accepting solvent such as DMSO to $CDCl_3$ solutions of the dendrimer allows for the identification of intramolecular H-bonded amide NH groups by ^{1}H NMR.[40,41] In general, a non-H-bonded amide will interact with the DMSO establishing S═O··HN intermolecular H-bonding interactions. These interactions are strongly concentration dependent, and thus non-H-bonded amide protons will experience downfield shifts which are dependent on the DMSO concentration. In contrast, strongly H-bonded amide NH will experience an upfield shift since their H-bonding is disrupted by the presence of DMSO.

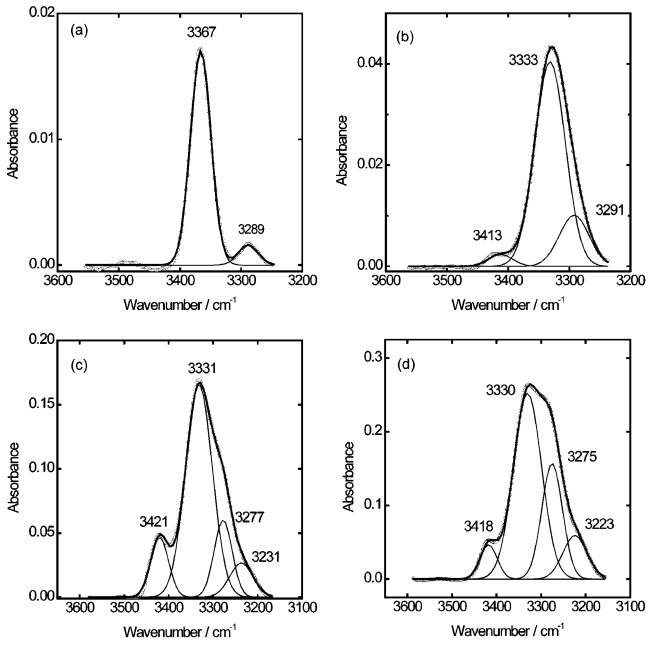

Figure 6. Deconvoluted NH bands of dendrimers (a) **G1**, (b) **G2**, (c) **G4**, and (d) **G6**. Two H-bonded bands are observed in **G1** which increases to three by the addition a non-H-bonding band in the 3415 cm^{-1} region in **G2** and then to four bands in higher generations **G3**−**G4** by the addition of a H-bonded band in the 3220−3230 cm^{-1} region.

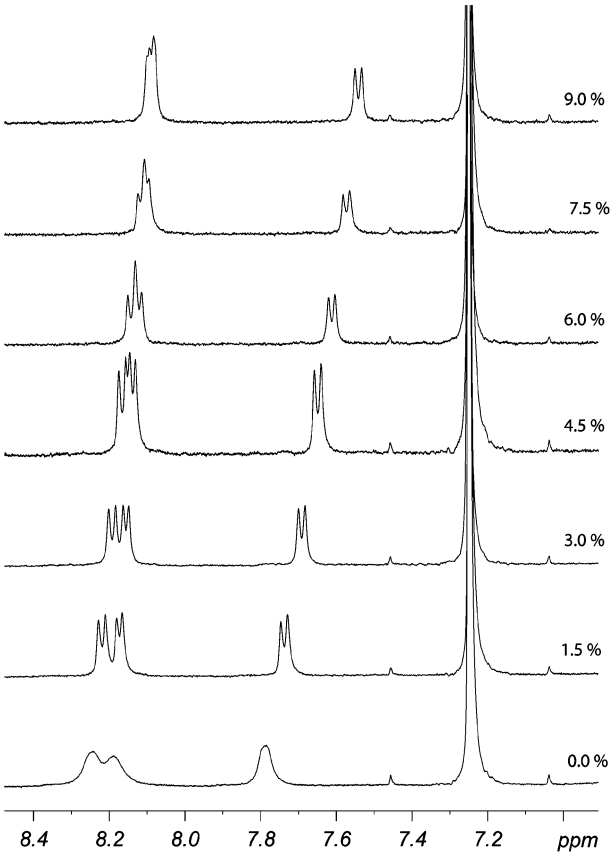

Figure 7. Effect of DMSO-d_6 addition to the amide NH to compound **G2** in $CDCl_3$.

Figure 7 shows the effect of addition of DMSO-d_6 to a solution of **G2**. All amide signals experience a slight upfield shift with increasing amounts of DMSO-d_6 added to the solution and sharpen to clear well-defined doublets. This is a result typical for systems in which all amides are involved intramolecular H-bonding. From the IR of **G1**−**G6**, we learned that

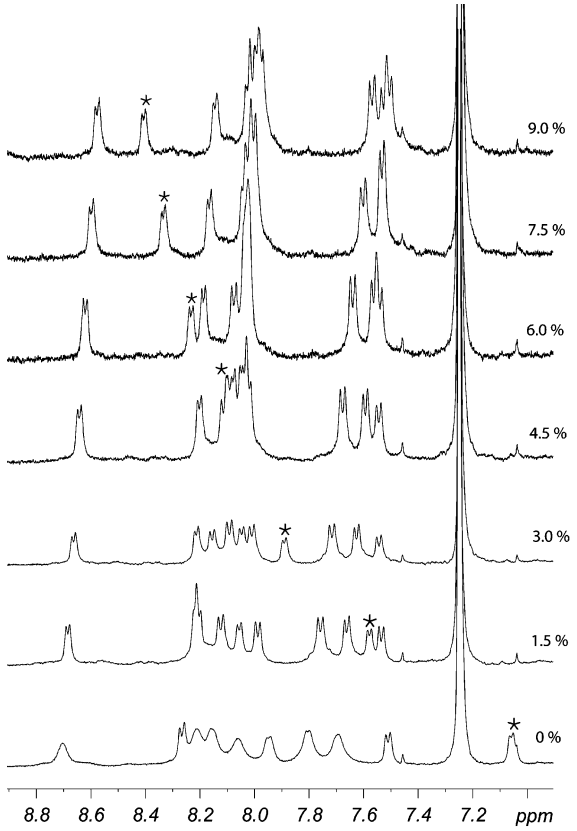

Figure 8. Effect of DMSO-d_6 addition to the amide NH to compound **G3** in $CDCl_3$. Non-H-bonded amide NH (shown by *) at δ 7.05 experiences a strong downfield shifted due to H-bonding with DMSO. Other amide resonances are shifted upfield due to a disruption of the H-bonding.

upon increasing generation the number of non-H-bonded amide NH increases. **G3** has such an amide proton. H-bonding interactions of such NH groups with DMSO-d_6 result in a downfield shift. Figure 8 shows the effect of DMSO-d_6 on the amide NHs of the **G3** in $CDCl_3$. Addition causes a strong downfield shift of a non- H-bonded amide NH at δ 7.05, while the peak positions of all other amide NH experience an upfield shift due to the disruption of the inherent H-bonding in the peptide dendrimer.

Effects of Dendritic Encapsulation on the Redox Properties of Disubstituted Ferrocene Peptides. The effect of the dendritic sphere on the redox properties of dendrimers **G1**−**G6** were investigated in solution by cyclic voltammetry (CV). A representative CV and a graph of $E_{1/2}$ vs dendrimer generation are shown in Figure 9.

G1−**G4** display quasi-reversible redox behavior, as is suggested by a peak separation ΔE_p of 74−150 mV and peak current ratios which are close to unity. Importantly, the $E_{1/2}$ shows a dependence on the dendritic generation and is shifted from $E_{1/2}$ 872(9) mV for **G1** to 776(3) mV for **G4**. Although cathodic shifts were also observed for the monosubstituted analogues, the magnitude of the shifts to lower potential is surprisingly large in the disubstituted systems.[10] We rationalize the magnitude of the shifts by changes that occur in the Cp−Fe−Cp torsion angle. Both the changes in the torsion and lack of H-bonding of the proximal Fc−amide will affect the redox potential of the central Fc moiety. Our observed shifts are also in contrast to those observed for some other disubstituted Fc dendrimers. Disubstituted Fc−benzyl ether dendrimers[7,8] and disubstituted Fc−carbohydrate dendrimers[9] exhibit shifts to higher potential with increasing generations. Our results are

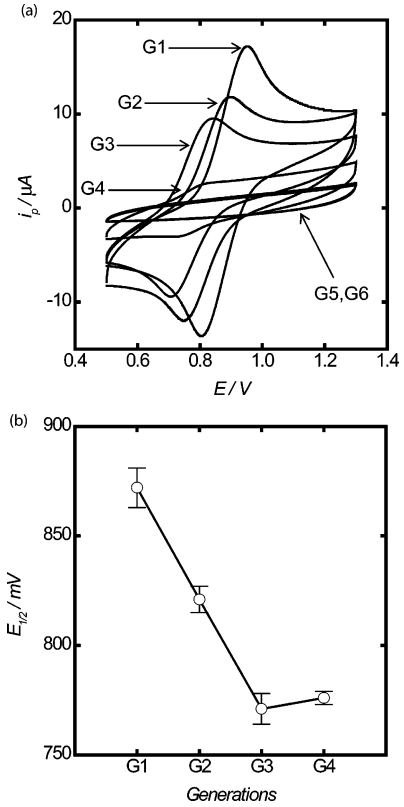

Figure 9. (a) CV and (b) graph of $E_{1/2}$ vs dendrimer generation. CV was recorded for 0.5 mM solutions of dendrimers in $CHCl_3$ **G1**−**G6** using a glassy carbon electrode working electrode, a Pt counter electrode, and a Ag/AgCl reference electrode, 0.2 M TBAP; scan rate of 100 mV·s^{-1}, $T = 23 \pm 1$ °C.

compatible with Kaifer's systems.[3] In Kaifer's work, a central Fc core is encapsulated by Behera's amine. With increasing dendrimer generation and size, the $E_{1/2}$ of the central Fc group is shifted to lower potential, making it easier to oxidize the Fc core. The observed shift to lower potential for our dendrimers **G1**−**G4** is consistent with a back-folded conformation adopted by the dendrimers at higher generations which is brought about by the increasing H-bonding and dendritic shielding of the Fc environment.[42,43]

Importantly, the peak current drastically reduces with increasing generations, which indicate shielding of the Fc group by the dendrimer. The decrease in the peak current with increasing generations and the lack of redox activity in **G5** and **G6** can be related to the increased steric hindrance from the dendritic shealth and to a lesser extent to the decrease in the diffusion coefficient of the dendrimers. The dendrons surrounding the Fc core will result in a decrease in the peak current and will significantly slow down the electron-transfer kinetics since the tunneling distance between the electrode surface and the Fc core increases significantly.

The redox activity of these dendrimers in solution involves diffusion to the electrode, and the electrons would have to tunnel from the redox center to the electrode through the dendritic sheath.

Since the rate of electron transfer is related to the donor−acceptor distance, it can be expected that an increasing dendrimer size will influence the kinetics of the electron-transfer process and thus of the observed solution electrochemistry.

The diffusion coefficients in Table 4 were obtained from pulse gradient spin-echo (PGSE) NMR measurements using the Stejskal−Tanner relationship (see Supporting Information). This allows us to obtain the hydrodynamic radius of the dendrimers,

Table 4. Electrochemical and Other Physical Data of Disubstituted Fc−Peptide Dendrimers[a]

	G1	G2	G3	G4	G5	G6
$E_{1/2}$/mV	872 (9)	831 (6)	771 (7)	776 (3)		
ΔE_p/mV	149 (8)	152 (5)	122 (6)	75 (5)		
i_c/i_a	1.0	1.1	1.2	1.1		
D_0 (NMR)	13.6 (0.2)	9.7 (0.2)	7.0 (0.1)	0.5 (0.1)	0.3 (0.1)	0.3 (0.1)
r_h/Å (NMR)	0.4	0.5	0.7	10.0	18.0	19.0
diameter[b]/Å	13	16	22	28	33	41

[a] 0.5 mM dendrimers at glassy carbon working electrode vs Ag/AgCl, 0.2 M TBAP, 100 mV s^{-1} at 23 ± 1 °C; NMR: $D_0 \times 10^5$ cm^2 s^{-1}, standard deviation in parentheses. [b] Molecular diameter obtained from molecular modeling.

as was described before for the monosubstituted Fc dendrimers.[10] As expected, with increasing dendrimer generation, the dendrimer increases in mass and size and the diffusion coefficient decreases in magnitude. Using the diffusion coefficient D_0, we are able to obtain the hydrodynamic radius of the dendrimer, i.e., the molecular dimensions, and are able to compare them with those obtained from molecular modeling. The values for the hydrodynamics radius of **G1**−**G6** and their diameters obtained from molecular modeling are summarized in Table 4. Inspection of the values shows that the diameters of the dendrimers obtained from molecular modeling agree well with the experimental values derived from the diffusion coefficient obtained by PGSE-NMR measurements.

Conclusions

Disubstituted Fc-functionalized peptide dendrimers were synthesized by the convergent method of synthesis and characterized by spectroscopic techniques. These dendrimers constitute well-defined structural entities, stabilized by the formation of strong intramolecular H-bonding. The proximal amide protons of Fc-CONH of lower generations **G1** and **G2** are involved in intramolecular H-bonding as would be expected for systems adopting a 1,2′-conformation, and therefore addition of DMSO will disrupt the intramolecular H-bonding pattern. Higher generations, however, have non-H-bonded amides NHs which are accessible and are influenced by DMSO addition. This is in contrast to the monosubstituted analogues which showed Fc−CONH interactions with DMSO in the lower generations but are inaccessible for interactions in higher generations. Corroborating evidence is provided by the CD studies, which indicate changes in the Fc conformation for higher generations away from the H-bonded 1,2′-conformation to a more open accessible conformation. We assume that these conformational changes are the result of increase in size in the glutamic acid dendrimer. As the dendrimers increase in size, the central Fc group can no longer maintain the 1,2′-conformation and opens up to a 1,3′-conformation which does not possess the H-bonding interaction proximal to the Fc group. Molecular modeling studies essentially provide evidence for these structural changes and also show that the dendrimers adopt globular structures in higher generations as a result of the backfolding of the peptide onto itself. As a consequence, the $E_{1/2}$s for **G1**−**G4** shift cathodically as a function of increasing dendrimer generation. This indicates that the oxidation of the Fc core becomes more favorable, similar to observations made by Kaifer and co-workers. Molecular modeling indicates complete encapsulation for **G5** and **G6**. Indeed, the solution electrochemistry of **G5** and **G6** does not show any Faradaic activity.

Acknowledgment. This work was partly supported by the National Science and Engineering Research Council of Canada (NSERC), the Canada Foundation for Innovation (CFI), and the

Saskatchewan Innovation Fun (SIF). H.-B.K. is the Canada Research Chair in Biomaterials. The Saskatchewan Structure Science Centre (SSSC) is acknowledged for providing access to all necessary instrumentation. Ken Thoms and Anas Lataifeh, Chemistry Department, University of Saskatchewan, are also acknowledged for carrying out the MS experiments.

Supporting Information Available: ^{1}H NMR spectra, DMSO-d_6 exchange experiments, tables of NMR, UV, and CD data, experimental details on PGSE NMR, and fit of **G1**−**G6** self-diffusion data to the Stejskal−Tanner equation. This material is available free of charge via the Internet at http://pubs.acs.org.

References and Notes

(1) Astruc, D.; Daniel, M.-C.; Ruiz, J. *Chem. Commun.* **2004**, 2637−2649.
(2) Smith, D. K.; Diederich, F. *Chem.*−*Eur. J.* **1998**, *4*, 1353−1361.
(3) Cardona, C. M.; Kaifer, A. E. *J. Am. Chem. Soc.* **1998**, *120*, 4023−4024.
(4) Wang, Y.; Cardona, C. M.; Kaifer, A. E. *J. Am. Chem. Soc.* **1999**, *121*, 9756−9757.
(5) Cardona, C. M.; McCarley, T. D.; Kaifer, A. E. *J. Org. Chem.* **2000**, *65*, 1857−1864.
(6) Stone, D. L.; Smith, D. K.; McGrail, P. T. *J. Am. Chem. Soc.* **2002**, *124*, 856−864.
(7) Jayakumar, K. N.; Thayumanavan, S. *Tetrahedron* **2005**, *61*, 603−608.
(8) Jayakumar, K. N.; Bharathi, P.; Thayumanavan, S. *Org. Lett.* **2004**, *6*, 2547−2550.
(9) Ashton, P. R.; Balzani, V.; Clemente-León, M.; Colonna, B.; Credi, A.; Jayaraman, N.; Raymo, F. M.; Stoddart, J. F.; Venturi, M. *Chem.*−*Eur. J.* **2002**, *8*, 673−684.
(10) Appoh, F. E.; Thomas, D. S.; Kraatz, H.-B. *Macromolecules* **2005**, *38*, 7562−7570.
(11) van Staveren, D. R.; Metzler-Nolte, N. *Chem. Rev.* **2004**, *104*, 5931−5985.
(12) van Staveren, D. R.; Weyhermüller, T.; Metzler-Nolte, N. *Dalton Trans.* **2003**, *2*, 210−220.
(13) Moriuchi, T.; Nomoto, A.; Yoshida, K.; Ogawa, A.; Hirao, T. *J. Am. Chem. Soc.* **2001**, *123*, 68−75.
(14) Herrick, R. S.; Jarret, R. M.; Curran, T. P.; Dragoli, D. R.; Flaherry, M. B.; Lindyberg, S. E.; Slate, R. A.; Thomton, L. C. *Tetrahedron Lett.* **1996**, *37*, 5289−5292.
(15) Vinogradov, S. A.; Lo, L.-W.; Wilson, D. F. *Chem.*−*Eur. J.* **1999**, *5*, 1338−1347.
(16) Vinogradov, S. A.; Wilson, D. F. *Chem.*−*Eur. J.* **2000**, *6*, 2456−2461.
(17) de Hatten, X.; Weyhermueller, T.; Metzler-Nolte, N. *J. Organomet. Chem.* **2004**, *689*, 4856−4867.
(18) Ranaganathan, D.; Kurur, S. *Tetrahedron Lett.* **1997**, *38*, 1265−1268.
(19) Jiang, H.; Leger, J.-M.; Dolain, C.; Guionneau, P.; Huc, I. *Tetrahedron* **2003**, *59*, 8365−8374.
(20) Boas, U.; Karlsson, A. J.; de Waal, B. F. M.; Meijer, E. W. *J. Org. Chem.* **2001**, *66*, 2136−2145.
(21) Kirin, S. I.; Wissenbach, D.; Metzler-Nolte, N. *New J. Chem.* **2005**, *29*, 1168.
(22) Grossel, M. C.; Goldspink, M. R.; Hriljac, J. A.; Weston, S. C. *Organometallics* **1991**, *10*, 851−860.
(23) Moriuchi, T.; Nomoto, A.; Yoshida, K.; Hirao, T. *J. Organomet. Chem.* **1999**, *589*, 50−58.
(24) Avent, A. G.; Bedford, R. B.; Chaloner, P. A.; Dewa, S. Z.; Hitchcock, P. B. *J. Chem. Soc., Dalton Trans.* **1996**, 4633−4638.
(25) Xu, Y.; Saweczko, P.; Kraatz, H.-B. *J. Organomet. Chem.* **2001**, *637*−*639*, 335−342.
(26) Cavallo, L.; Fraternalli, F. *Chem.*−*Eur. J.* **1998**, *4*, 927−934.
(27) Naylor, A. M.; Goddard, W. A.; Kiefer, G. E.; Tomalia, D. A. *J. Am. Chem. Soc.* **1989**, *111*, 2339−2341.
(28) Lescanec, R. L.; Muthukumar, M. *Macromolecules* **1990**, *23*, 2280−2288.
(29) Gung, B. W.; Zhu, Z. *Tetrahedron* **1996**, *37*, 2189−2192.
(30) Gung, B. W.; Zhu, Z. *J. Org. Chem.* **1997**, *62*, 6100−6101.
(31) Gellman, S. H.; Dado, G. P.; Liang, G.; Adams, B. R. *J. Am. Chem. Soc.* **1993**, *113*, 1164−1173.
(32) Haris, P. I. In *Infrared Analysis of Peptides and Proteins: Principles and Applications*; Singh, B. R., Ed.; American Chemical Society: Washington, DC, 2000; pp 54−95.
(33) Hollosi, M.; Majer, Z. S.; Ronal, A. Z.; Magyar, A.; Medzihradszky, K.; Holly, S. *Biopolymers* **1994**, *34*, 177−186.
(34) Lopez de la Paz, M.; Ellis, G.; Perez, M.; Perkins, J.; Jimenez-Barbero, J.; Vicent, C. *Chem.*−*Eur. J.* **2002**, 840−855.
(35) Kuhn, L. P.; Schleyer, P. V. R.; Baitinger, J. W.; Eberson, L. *J. Am. Chem. Soc.* **1964**, *86*, 650−658.
(36) Brimacombe, J. S.; Foster, A. B.; Stacey, M.; Whiffen, D. H. *Tetrahedron* **1958**, *4*, 351−360.
(37) Rabolt, J. F.; Moore, W. H.; Krimm, S. *Macromolecules* **1977**, *10*, 1065−1074.
(38) Lee, S.-H.; G.; M. N.; Krimm, S. *Biopolymers* **1999**, *49*, 195−207.
(39) Bridelli, M. G.; Capelletti, R.; Maraia, F.; Mora, C.; Pirola, L. *J. Phys. D: Appl. Phys.* **2002**, *35*, 1039−1048.
(40) Maji, S. K.; Banerjee, R.; Velmurugan, D.; Razak, A.; Fun, H. K.; Banerjee, A. *J. Org. Chem.* **2002**, *67*, 633−639.
(41) Maji, S. K.; Haldar, D.; Bhattacharyya, D.; Banerjee, A. *J. Mol. Struct.* **2003**, *646*, 111−123.
(42) Chasse, T. L.; Yohannan, J. C.; Kim, N.; Li, Q.; Li, Z.; Gorman, C. B. *Tetrahedron* **2003**, *59*, 3853−3861.
(43) Chasse, T. L.; Sachdeva, R.; Li, Z.; Petrie, R. J.; Gorman, C. B. *J. Am. Chem. Soc.* **2003**, *125*, 8250−8254.

MA060525X